On the Feasibility of Using Passive mm-Wave Imaging for Marine Litter Detection at the W-band

Mário Vala*†, João M. Felício*‡, Tomás Soares da Costa*†, Nuno Leonor*§, Jorge R. Costa*¶, Paulo Marques*‖, António A. Moreira*†, Sérgio A. Matos *¶, Rafael F. S. Caldeirinha*§, Carlos A. Fernandes *†, Nelson J. G. Fonseca **, Peter de Maagt **

*Instituto de Telecomunicações, Portugal

†Instituto Superior Técnico, Universidade de Lisboa, 1049-001, Lisbon, Portugal

‡Centro de Investigação Naval, Escola Naval, Instituto Universitário Militar, 2810-001 Almada, Portugal

§Polytechnic of Leiria, Leiria, Portugal

¶Departamento de Ciências e Tecnologias da Informação, Instituto Universitário de Lisboa (ISCTE-IUL), 1649-026 Lisbon, Portugal

‖Instituto Superior de Engenharia de Lisboa (ISEL), 1959-007, Lisbon, Portugal

**Antenna and Sub-Millimetre Wave Section, European Space Agency (ESA), Noordwijk, The Netherlands

mario.vala@co.it.pt

***Abstract*—Large research effort is appearing in the literature on remote detection of plastic marine litter, using optical instruments, and lately microwaves. We present here a feasibility study of passive mm-wave imaging (PMMWI) for the same goal. Several measurements were taken in a controlled pool environment both in static and agitated water conditions using a W-band radiometer to assess the influence of plastic on the radiometric response. Different sized plastic bottles and concentrations were studied to verify its influence on the results provided by the radiometer. For each measurement, references of still water were taken to correct eventual errors due to equipment drifts in terms of gain and noise. Preliminary results show that it is possible to detect differences in the radiometers output voltage when plastic is present or the water is agitated or both and, thus, PMMW imaging seems to be a promising technology for remote detection of floating plastics.**

***Index Terms*—Marine plastics, PMMW, passive radar, radiometer, W-band.**

I. Introduction

The increase of marine litter in the last decades has been a rising concern worldwide, as it can be harmful for both ocean wildlife and potentially to humans. In [1], a review of the impacts of plastic marine debris in ocean life was carried out, yielding a total of 362 impacts due to debris. From these 362 perceived impacts, 87% were associated with plastic debris, leading to the death of several species (from fishes to marine mammals, sea birds, and others) being ingestion, entanglement and smothering the principal cases.

The plastic present in the ocean may have two sources, land-based and marine, corresponding to 80% and 20% of total marine plastic debris, respectively [2]. The pollution from marine sources are mostly resulting from fishing fleets that leave behind fishing nets, lines, ropes and abandoned vessels. A total of 640 ktons of discarded fishing gear is estimated to be added to the ocean each year, contributing to approximately 10% of total marine debris [3]. The land-based pollution side, which is the major contributor to ocean pollution with 80% of total plastic debris, results mostly from densely populated or industrialized areas, majorly due to littering, plastic bag usage and solid waste disposal [2].

These alarming results call for the development of methods that would allow the detection of marine litter in deep sea areas. Satellite based detection represents a very enticing option as satellites can cover large areas of ocean and reach almost every part of the sea during their trajectory around the planet. One of such methods may include the usage of satellites equipped with radio frequency (RF) equipments as RF signals are less affected by weather conditions such as clouds or rain that may prevent other methods of detection from working, therefore enabling the continuous monitoring of floating plastics.

Since marine litter detection is still a somewhat new research topic, currently there is still not a clear solution that allows remote detection of plastics in the ocean. Nevertheless, some studies in the RF domain were already presented in the literature [4], [5], [6]. A review of marine litter detection through remote sensing published in 2021 [6] showed that regarding RF detection, the studies performedaimed at the detection of microbial biofilms associated with marine bacteria and not directly macroplastics. From this study [6], it can be seen that all the measurements performed at MW frequencies were either in the C-band (4 to 8 GHz) or at X-band (8 to 12 GHz) and with resolutions between 3 and 30 m.

However, a technique that has yet to be explored for these applications is the passive mm-wave (PMMW) imaging based technique. This passive technique aims at detecting the natural electromagneetic emission from matter in a given band. Radiometers are generally used for that and have operated in a large variety of scenarios. Even though PMMW imaging has been used for Earth observation [7], [8], [9], such as soil moisture, sea surface salinity, sea ice thickness, etc, to the authors' knowledge, there is no literature on the use of this technique for marine litter detection and, thus, the novelty of

this work.

This is the motivation for this feasibility study, which will be conducted for a very controlled small scale scenario. Moreover, the frequency band used herein is the W-band (75 - 110 GHz) which corresponds to a moderate transparency window of the Earth's atmosphere, as required for satellite-based applications as seen in [10].

This paper is structured as follows: in Section II, some theoretical foundations for radiometry are laid out; in Section III the setup and measurement results are presented and analyzed and lastly in Secion IV the conclusions of the work are drawn as well as possible future work on this front.

II. Passive mm-wave imaging

All objects emit radiation to a degree that is characterized by the object's emissivity (ε) [11] in a way that a perfect radiator and a perfect absorber present emissivities of 1 and 0, respectively. This attribute is dependent on several characteristics of the measurement, such as polarization and angle of observation, as well as properties of the materials being analyzed, such as dielectric constant and surface roughness.

Even though radiometers are used to measure integrated noise power across the device bandwidth, it is common to express power in terms of an equivalent temperature called brightness temperature, T_B that corresponds to the temperature of a blackbody that would radiate the same power or an antenna temperature, T_A that is the temperature of a resistor that has the same output power of the receiving antenna [12]. The brightness temperature of an object can be related to its thermodynamic temperature T_O by the relation [11]:

$$T_B = \varepsilon \cdot T_O \tag{1}$$

Thus, the objective of a passive mm-wave (radiometric) measurement is to relate the antenna temperature to the brightness temperature of the object in question. However, to achieve this, sufficient resolution in the antenna temperature measurement is of utter importance.

In a radiometer system, the output power (in W) can be calculated using the formula:

$$P = k \cdot B \cdot G \cdot (T_A + T_N), \tag{2}$$

where k is the Boltzmann's constant ($1.38 \times 10^{-23} J/K$), G is the gain of the radiometer amplifier and B is the bandwidth of the receiver. In this equation another temperature is present, T_N, that corresponds to the noise temperature, as the radiometer components will also generate noise. These two are additive and cannot be separated. However, there is no problem with radiometric stability if the values of B, G and T_N are constant [13].

As explained previously, the signals being measured are noise signals, that have a well-defined mean with random fluctuations. These fluctuations can be reduced by averaging or integrating, leading to a sensitivity that can be defined as (3):

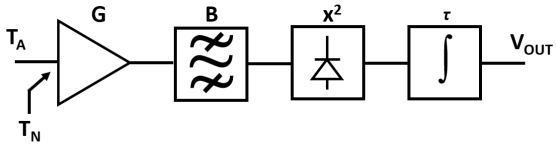

Fig. 1: Total power radiometer block diagram (based on [12]).

$$\Delta T = \frac{T_A + T_N}{\sqrt{B \cdot \tau}}, \tag{3}$$

where τ is the integration time. The most straightforward radiometer configuration, and the one that will be used for the measurements presented in this study, is the total power integrated by the radiometer [12], for which the block diagram is presented in Fig.1.

The constituents of the total power radiometer are as follows: the gain of the radiometer is symbolized by an amplifier with gain G, the selectivity in frequency with a band-pass filter with bandwidth B, a square-law detector and an integrator. The output voltage of the power detector will be proportional to the input power (and input temperature). Lastly, the signal from the detector is smoothed by the integrator to reduce fluctuations of the output. Thus, the output voltage of a total power radiometer can be calculated as follows [12]:

$$V_{OUT} = c \cdot (T_A + T_N) \cdot G, \tag{4}$$

where c is a constant. As can be seen from the expression, the output voltage is dependent on the noise temperature and gain of the radiometer. As these parameters might not be considered stable enough, this type of radiometer might not be suitable depending on the accuracy requirements. It is very useful however, for measurements where frequent calibration and references are possible.

III. Results and analysis

In order to assess the impact of floating plastic on the response of a W-band radiometer in a small-scale controlled environment using PMMW imaging, a very simple setup was assembled outside our laboratory facilities, where the radiometer antenna was pointed towards a pool filled with water, with a height of 20 cm as shown in Fig. 2. The objective of this study was to place plastic objects (in this case water bottles) in the antenna's footprint and verify if there was a difference between the radiometer output with these bottles in contrast to the case where there was only water in the antenna footprint.

For these measurements, a linearly polarized SGH-10-24G antenna was connected to a Farran PMMW-10-0001 radiometer [14] operating at W-band (between 75 and 110 GHz). The antenna presents a 25 dBi gain at the desired frequency band and a 3 dB beamwidth of 9° and 10° in the E- and H-planes, respectively. The radiometer has a sensitivity of 0.4 K and a differential voltage output. This radiometer consists of a low noise front-end with high-gain, followed by a broadband

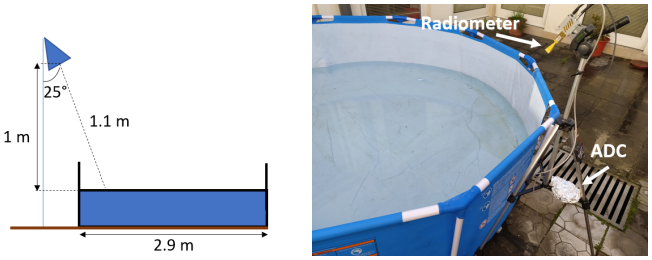

(a) (b)

Fig. 2: PMMW measurement setup: a) geometry and b) photograph.

Fig. 3: Radiometric measurement with various bottles.

W-band detector. The signal is then conditioned in a video amplifier to give an output level depending on the brightness temperature of the object. To achieve this sensitivity, the radiometer integration time was defined to be (τ) of 120 μs. In order to retrieve the data obtained by the radiometer, a NI USB-6008 ADC [15] was connected to it. This ADC allowed for the retrieval of differential radiometer output with 12 bits with a maximum sample rate of 10 kSamples/s.

The antenna was placed 1 m above the water level with a 25° inclination from nadir, yielding to a distance of 1.1 m to the water surface. This geometry coupled to the antenna pattern leads to a footprint of 19 by 20 cm. It is important to note that for each measurement presented in this section several references were taken to have a reference that took place near in time to the measurement in plastic. This had to be done due to the fact that the output results for the same scenario could be different depending on external factors, such as temperature, time of day, etc, that would affect the characteristics of the radiometer (gain and noise temperature) as explained in Section II. These reasons would explain the differences observed between the references for the different measurements.

In the first measurement, several static bottles were left floating on the water, held in place by a string attached to the outer ring of the pool, as seen in Fig. 3. The number of bottles in this first measurement was high to ensure that the plastic would cover the majority of the antenna footprint.

To test whether the insertion of plastic in the setup affected the output of the radiometer, reference measurements (without

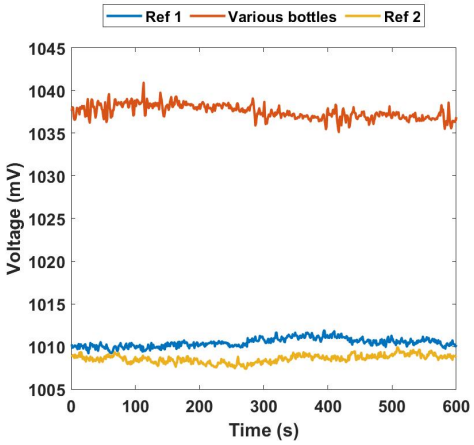

Fig. 4: Radiometer results when placing floating water bottles in the pool.

plastic) were taken before and after the insertion of the plastic bottles. The outputs of the radiometer were recorded during 10 minutes for each measurement and the results are presented in Fig. 4.The results presented herein correspond to the averaging of the 10 kSamples taken each second.

When analyzing these results, both references are similar and constant during the measurement, being the output voltage around 1010 mV. When the bottles were introduced, there was an increase in the output voltage to 1036 mV. When the bottles were removed, the brightness temperature returned to its initial level.

The objective of the second measurement was to verify if the plastic quantity would have an effect on the results given by the radiometer. To test this, a measurement with various bottles and with only one 1.5 L bottle was taken, leading to the results depicted in Fig. 5. Another change from the previous setup was that the bottles were not tied so tightly than they were in the previous scenario, so they can move during the acquisition window, which led to some variation of the voltage over the 10 minute period. For this set of measurements, three references were taken: one before placing the bottles, one between both measurements and one after. Similarly to the previous case, all the references converge which seems to confirm that the alteration in output voltage is due to the insertion of plastic. However, for this case, average output voltages of 1023 mV and 1018 mV were obtained for the cases of various bottles and one 1.5 L bottle, respectively. The results in Fig. 5 show a stronger variation over time for the plastic case with various bottles. This indicates that the actual distribution has an impact on the response as results in Fig. 4 with tightly fixed bottles showed a very stable response.

Up to this point, all the measurements were taken with still water. It is relevant to evaluate if the presence of waves changes the previous previous conclusion. To do this, some waves were generated in the pool. Fig. 6 compares the radiometer results obtained with waves without target (Waves), without waves and without target (Ref 1 to Ref 3), and without

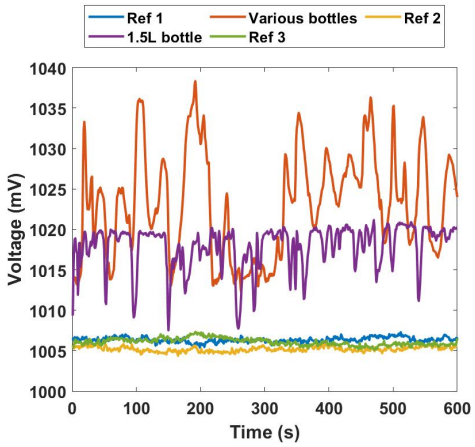

Fig. 5: Radiometer results with different plastic concentrations.

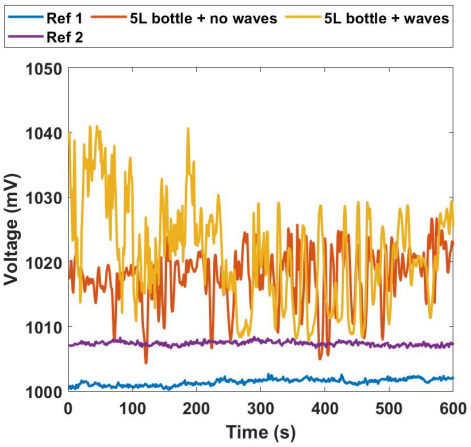

Fig. 7: Radiometer measurements of the combined effect of waves with plastic presence.

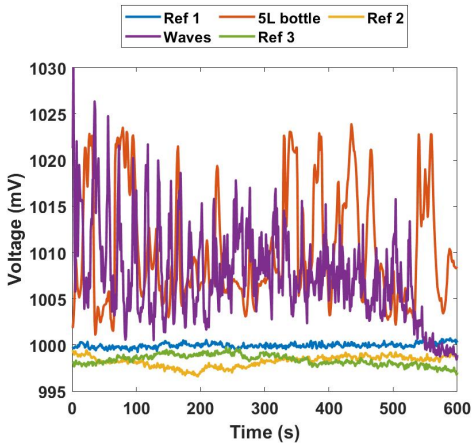

Fig. 6: Comparison of radiometer results when considering water surface with waves and a 5 L plastic bottle in still water.

waves but with a 5L bottle. Again for this case, three reference measurements were taken in the same way as the previous case, being all similar as well. The waves were highest at the beginning of the measurement and slowly started to diminish in height, leading to the change in voltage amplitude up to the 500 s mark. At this point, the generation of waves stopped completely, leading to a decrease in voltage that trended to the reference case as the waves attenuated. These results show that the impact of a 5 L bottle is similar to the impact of water dynamic, which can be a deterrent to the usage of this method as a satellite-based marine litter detection.

These results led to the last measurement, where the combined effect of the waves with the presence of plastic was compared with the presence of plastic in still water. For this, a bottle of 5 L was used again, yielding the results of Fig. 7. In this case, only two references were taken: one before the measurements and one after. The water was agitated only until the time instant of 220 s. Up to this point, it is possible to see that there is a slight increase in the voltage and that after, the results trend to the case where only the 5 L bottle is present in still water. The average voltage output until the point where the waves stopped was of 1027 mV. After this point the voltage decreased to have a mean of 1018 mV which coincides with the average of the 10 minute measurement without waves, indicating that the effects of the waves and the presence of the bottles are cumulative.

IV. Conclusions

In this paper, the feasibility of using a passive mm-wave imaging techniques to detect floating marine litter at W-band is analyzed. Preliminary measurements in a controlled environment using a radiometer hint that it is possible to distinguish when there is plastic in the antenna footprint in still water. Moreover, the output voltage was shown to increase with the increase of plastic, despite the water conditions.

However, the dynamics of the water also influence the results, as there was a visible increase in the radiometers output voltage when water was agitated that was similar to the increase observed when placing a 5 L bottle in static water in front of the antenna. This increase was shown to be cumulative when both the water is agitated and a 5 L bottle is present.

Future work will entail the implementation of a hot/cold calibration system to ensure that all the measurements are taken with reference to these values and, ultimately, to retrieve the actual brightness temperature for effective object detection and identification. Also, additional measurements at larger distances are also planned. However, a very high gain antenna is needed in order to have a relatively small footprint and sufficient gain, and, thus, sufficient dynamic range, to detect brightness temperature variations emanated by distant targets.

Acknowledgments

This research was partially supported by Fundação para a Ciência e a Tecnologia-FCT/MCTES and co-funded by FEDER – PT2020 partnership agreement under project UIDB/50008/2022, by FCT PHD grants 2020.0855.BD

and UI/BD/151090/2021, and by ESA under contract nº 4000136690/21/NL/GLC/ov - MARES project.

REFERENCES

[1] C. M. Rochman, M. A. Browne, A. J. Underwood, J. A. van Franeker, R. C. Thompson, and L. A. Amaral-Zettler, "The ecological impacts of marine debris: unraveling the demonstrated evidence from what is perceived," *Ecology*, vol. 97, no. 2, pp. 302–312, feb 2016.

[2] W. LI, H. TSE, and L. FOK, "Plastic waste in the marine environment: A review of sources, occurrence and effects," *Science of The Total Environment*, vol. 566-567, pp. 333–349, oct 2016.

[3] T. P. Good, J. A. June, M. A. Etnier, and G. Broadhurst, "Derelict fishing nets in puget sound and the northwest straits: Patterns and threats to marine fauna," *Marine Pollution Bulletin*, vol. 60, no. 1, pp. 39–50, jan 2010.

[4] N. Davaasuren, A. Marino, C. Boardman, M. Alparone, F. Nunziata, N. Ackermann, and I. Hajnsek, "Detecting microplastics pollution in world oceans using sar remote sensing," in *IGARSS 2018 - 2018 IEEE International Geoscience and Remote Sensing Symposium*. IEEE, jul 2018.

[5] S. P. Garaba and H. M. Dierssen, "An airborne remote sensing case study of synthetic hydrocarbon detection using short wave infrared absorption features identified from marine-harvested macro- and microplastics," *Remote Sensing of Environment*, vol. 205, pp. 224–235, feb 2018.

[6] P. M. Salgado-Hernanz, J. Bauzà, C. Alomar, M. Compa, L. Romero, and S. Deudero, "Assessment of marine litter through remote sensing: recent approaches and future goals," *Marine Pollution Bulletin*, vol. 168, p. 112347, jul 2021.

[7] N. J. Rodriguez-Fernandez, A. Mialon, O. Merlin, C. Suere, F. Cabot, A. Khazaal, J. Costeraste, B. Palacin, R. Rodriguez-Suquet, T. Tournier, T. Decoopman, E. Anterrieu, M. Colom, J.-M. Morel, Y. H. Kerr, B. Rouge, J. Boutin, G. Picard, T. Pellarin, M. J. Escorihuela, A. A. Bitar, and P. Richaume, "SMOS-HR: A high resolution l-band passive radiometer for earth science and applications," in *IGARSS 2019 - 2019 IEEE International Geoscience and Remote Sensing Symposium*. IEEE, jul 2019.

[8] S. Pelyushenko, "Microwave radiometer system for the detection of oil slicks," *Spill Science & Technology Bulletin*, vol. 2, no. 4, pp. 249–254, jan 1995.

[9] J. T. Johnson, K. C. Jezek, G. Macelloni, M. Brogioni, L. Tsang, E. P. Dinnat, J. P. Walker, N. Ye, S. Misra, J. R. Piepmeier, R. Bindlish, D. M. LeVine, P. E. OaNeill, L. Kaleschke, M. J. Andrews, C. Yardim, M. Aksoy, M. Durand, C.-C. Chen, O. Demir, A. Bringer, J. Z. Miller, S. T. Brown, R. Kwok, T. Lee, Y. Kerr, D. Entekhabi, J. Peng, A. Colliander, S. Chan, J. A. MacGregor, B. Medley, R. DeRoo, and M. Drinkwater, "Microwave radiometry at frequencies from 500 to 1400 MHz: An emerging technology for earth observations," *IEEE Journal of Selected Topics in Applied Earth Observations and Remote Sensing*, vol. 14, pp. 4894–4914, 2021.

[10] M. Miacci and C. F. Angelis, "Ground-based microwave radiometer calibration: an overview," *Journal of Aerospace Technology and Management*, vol. 10, jul 2018.

[11] L. Yujiri, M. Shoucri, and P. Moffa, "Passive millimeter-wave imaging," *IEEE Microwave Magazine*, vol. 4, no. 3, pp. 39–50, sep 2003.

[12] N. Skou and D. Vine, *Microwave Radiometer Systems, Design and Analysis*. Artech House, 2006.

[13] M. Šostronek, Z. Matoušek, B. Lakota, and M. Matejček, "W-band direct detection radiometer model," in *2015 International Conference on Applied Electronics (AE)*, 2015, pp. 221–224.

[14] "Pmmw-10-0001 radiometer datasheet," last acessed on 10/10/2022. [Online]. Available: https://farran.com/wp-content/uploads/2020/12/PMMW-10-0001.pdf

[15] "National instruments usb-6008 analog to digital converter," last acessed on 10/10/2022. [Online]. Available: https://www.ni.com/docs/en-US/bundle/usb-6008-specs/page/specs.html